PCCP

Theoretical modelling of the low quantum yield observed in an Eu(III) triple helical complex with a tridentate aromatic ligand

F. R. Gonçalves e Silva,*[a] R. Longo,[b] O. L. Malta,[b] C. Piguet[c] and J.-C. G. Bünzli[a]

[a] *Institute of Inorganic and Analytical Chemistry, University of Lausanne, BCH, CH-1015 Lausanne, Switzerland*
[b] *Departamento de Química Fundamental-UFPE, 50670-901 Recife, PE-Brazil*
[c] *Department of Inorganic Chemistry, University of Geneva, CH-1211 Geneva-4, Switzerland*

Received 12th July 2000, Accepted 9th October 2000
First published as an Advance Article on the web 10th November 2000

The dramatic decrease in the quantum yield of the Eu-centred luminescence recently observed in going from $[Eu(NO_3)_3L(MeOH)]$ (2.8%) to the triple helical $[Eu(L)_3](ClO_4)_3$ complex (8.2×10^{-5}%) prompted us to perform a theoretical analysis in order to find out which parameter might be responsible for this quenching. In particular, we explore the influence of a resonance between a ligand-to-metal charge-transfer state (LMCT) and the $^1\pi\pi^*$ and/or $^3\pi\pi^*$ states on the emission quantum yield. A good agreement between the theoretical and experimental values is reached when high rates for non-radiative deactivation on the ligand are considered and, for the 1 : 3 complex, when a LMCT state close in energy to the ligand $^1\pi\pi^*$ state is taken into account. This type of modelling opens the way for a better predictability of the photophysical properties of luminescent europium-containing edifices.

Introduction

Co-ordination compounds of trivalent lanthanide ions with antenna chromophores, when irradiated with ultraviolet light absorbed by the ligands, exhibit an emission spectrum with narrow lines corresponding to 4f–4f intraconfigurational transitions.[1] This phenomenon is a consequence of intramolecular energy transfer between the ligand(s) and the 4f states. The luminescent properties of lanthanide complexes are being thoroughly investigated due to their practical applications as luminescent labels for fluoroimmunoassays.[2,3] Photophysical studies and theoretical calculations of energy transfer rates and quantum efficiencies have provided a reasonable understanding of the luminescence process in these compounds. However, several rate constants involved in the energy transfer mechanisms between the ligands and the lanthanide ions are still unknown and a rational design of lanthanide luminescent probes would gain in predictability, were these rate constants known.

In the present work we apply the methodology developed for the kinetic study of energy transfer processes to elucidate the dramatic decrease in the quantum yield of the Eu-centred luminescence observed in going from $[Eu(NO_3)_3L(MeOH)]$ to the triple helical $[Eu(L)_3](ClO_4)_3$ complex, where L = 2,6-bis(1-methyl-benzimidazol-2-yl)pyridine (Fig. 1). Upon ligand excitation, 10^{-3} M solutions in anhydrous acetonitrile display absolute quantum yields of 2.8 and 8.2×10^{-5}% respectively.[4] Since most of the photophysical parameters of these complexes are identified and since their crystal structure is determined, they are ideal models to test our theory.

Calculations of the emission quantum yield were carried out by using the theoretical models for ligand-to-rare earth ion energy transfer processes and numerical solutions of the rate equations.[5–7] Intersystem crossing and internal conversion rates in the ligand moieties of the complexes are not experimentally available, thus these rates were optimised in order to reproduce the experimental data. Since a possible quenching mechanism involving a low lying ligand-to-metal charge-transfer state (LMCT) has been invoked to explain the low quantum yield of the 1 : 3 complex,[4] we have also examined the influence of a LMCT state quasi-resonant with the ligand singlet and triplet states on the emission quantum yield.

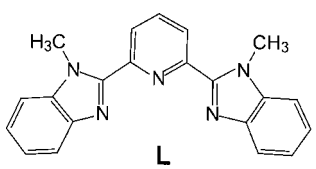

L

Fig. 1 Molecular structure of the L ligand molecule.

Quantum yield: theoretical aspects

In order to evaluate the theoretical quantum yield, it is necessary to know the molecular structure of the complexes, the ligand electronic structure, as well as the energy transfer rates and the temporal dependence of the populations of the ligand and lanthanide ion states. The known molecular structures of $[EuL(NO_3)_3(MeOH)]$[8] and $[Eu(L)_3](ClO_4)_3$,[9] determined by X-ray crystallography, were used to calculate the ligand electronic structure (transition energies and oscillator strengths) by the INDO/S-CI (intermediate neglect of differential overlap/spectroscopic-configuration interaction) method[10] implemented in the ZINDO program.[11] These results were used to calculate the energy transfer rates within the model described below. The overall ligand-to-Eu(III) energy transfer rate W_{ET} was obtained according to the theoretical model developed recently;[7,12] it is the sum of three contributions given by the following theoretical expressions:

$$W_{ET}^{mp} = \frac{2\pi}{\hbar}\frac{e^2 S_L}{(2J+1)G} F \sum_{\lambda} \gamma_{\lambda} \langle \alpha' J' \| U^{(\lambda)} \| \alpha J \rangle^2 \qquad (1)$$

which corresponds to the dipole–2^λ pole mechanism ($\lambda = 2$, 4 and 6),

$$W_{ET}^{dd} = \frac{2\pi}{\hbar}\frac{e^2 S_L}{(2J+1)GR_L^6} F \sum_{\lambda} \Omega_{\lambda}^{ed} \langle \alpha' J' \| U^{(\lambda)} \| \alpha J \rangle^2 \qquad (2)$$

 DOI: 10.1039/b005624n

corresponding to the dipole–dipole mechanism ($\lambda = 2$, 4 and 6), and

$$W_{ET}^{ex} = \frac{8\pi}{3\hbar}\frac{e^2(1-\sigma_0)^2}{(2J+1)R_L^4} F\langle \alpha' J' \| S \| \alpha J\rangle^2 \times \sum_m \left| \langle \phi | \sum_k \mu_z(k) s_m(k) | \phi' \rangle \right|^2 \quad (3)$$

corresponding to the exchange mechanism. In the above equations J represents the total angular momentum quantum number of the rare earth ion, α specifies a given 4f spectroscopic term, G is the degeneracy of the ligand initial state and S_L is the electric dipole strength associated with the ligand transition $\phi \rightarrow \phi'$. The quantities $\langle \| \| \rangle$ are reduced matrix elements of the unit tensor operators $\boldsymbol{U}^{(\lambda)}$[13] and R_L is the distance from the rare earth ion nucleus to the region of the ligand molecule where the ligand donor (or acceptor) state is localised.[12] In eqn. (3), S is the total spin operator of the rare earth ion, μ_z is the z component of the electric dipole operator and s_m ($m = 0, \pm 1$) is a spherical component of the spin operator, both for the ligand electrons, and σ_0 is a distance-dependent screening factor.[14] The matrix elements $\langle \phi | \sum_k \mu_z(k) s_m(k) | \phi' \rangle$ were calculated[14,15] from the molecular orbital wave functions given by the INDO/S-CI method.[16] Ω_λ^{ed} are the contributions of forced electric dipole to the intensity parameters defined in ref. 15. The quantities γ_λ and F are given by:

$$\gamma_\lambda = (\lambda+1)\frac{\langle r^\lambda \rangle^2}{(R_L^{\lambda+2})^2}\langle 3\|C^{(\lambda)}\|3\rangle^2(1-\sigma_\lambda)^2 \quad (4)$$

$$F = \frac{1}{\hbar\gamma_L}\sqrt{\frac{\ln 2}{\pi}}\exp\left[-\left(\frac{\Delta}{\hbar\gamma_L}\right)^2 \ln 2\right] \quad (5)$$

where $\langle r^\lambda \rangle$ is the radial expectation value of r^λ for 4f electrons, $\boldsymbol{C}^{(\lambda)}$ is a Racah tensor operator,[17] the σ_λ's are screening factors,[18,19] γ_L is the ligand state bandwidth at half-height and Δ is the difference between the donor and acceptor transition energies involved in the transfer process.

The selection rules that can be derived from the above equations are the following:[7,14] $J + J' \geqslant \lambda \geqslant |J - J'|$, for the mechanisms expressed by eqns. (1) and (2) and $\Delta J = 0, \pm 1$, for the exchange mechanism, eqn. (3), in both cases $J' = J = 0$ is excluded. For the ligand, the selection rules can be derived from the electric dipole strength S_L and the matrix element of the coupled operators μ_z and s_m in eqn. (3).

The numerical solution of the rate equations describing the kinetics of the 4f–4f luminescence was carried out according to the model developed in ref. 7. The normalised level populations, η_i, are described by a set of rate equations which have the general form:

$$\frac{d\eta_i}{dt} = -\sum_{\substack{j=1\\ j\neq i}}^{N} k_{ij}\eta_i + \sum_{\substack{j=1\\ j\neq i}}^{N} k_{ji}\eta_j \quad (6)$$

where the indices i and j indicate the energy levels of the compound involved in the energy transfer process; k_{ij} or k_{ji} correspond to the transition rates between levels i and j, or between states j and i, respectively and N is the total number of states involved in the energy transfer mechanism. In the steady state regime all the $d\eta_i/dt$ are equal to zero and the set of algebraic equations can be solved analytically in terms of the transition and transfer rates. In the present case, the rate equations were solved numerically by using the 4th order Runge–Kutta method with an adaptive integration step.[7] This set of coupled differential equations belongs to the initial value category, where the populations (η_i) at $t = 0$ were set equal to 1 for the ground state population and to zero for the other states. The total time of propagation was around 0.01 s and the initial step size was equal to the inverse of the largest transfer rate (approximately 10^{-9} s). The numerical solutions of the rate equations yield the time dependence of the energy level populations, which reach the steady-state regime after 10^{-6}–10^{-5} s. These steady-state populations were then used to calculate the emission quantum yield given by

$$q = \frac{A_T \eta_2}{\theta \eta_1} \quad (7)$$

where the sub-indices 1 and 2 indicate the ground state and the emitting level ($^5D_0$), respectively, in the complex, A_T is the sum of the coefficients of spontaneous emission for the $^5D_0 \rightarrow {}^7F_{0,1,2,4}$ transitions and θ is the pumping rate.

Results and discussion

The experimental energies of the transitions to the singlet and from the triplet states are presented in Table 1 together with their theoretical evaluation and with the theoretical oscillator strengths for the transitions to the singlet states. All these transitions have a $\pi^* \leftarrow \pi$ character with the initial states centered mainly on the benzyl and imidazole rings, whereas final states are centered on the pyridine rings. The near degeneracy of the two calculated singlet state transitions in $[Eu(L)_3]^{3+}$ is due to small geometrical differences between the two benzimidazole moieties of the ligands.[9] The experimental triplet state energies were obtained from the phosphorescence spectra measured at 77 K for the La^{3+} compounds.[4]

The experimental energies of the singlet and triplet states were used to set up the right part of the diagram shown on Fig. 2. In this model, ligand-to-metal energy transfer may occur through either the singlet or triplet ligand states to several 4f states that compel with the selection rules discussed above. However, only five 4f levels possess appropriate resonance conditions with the ligand excited states: $^5D_0$, $^5D_1$, $^5D_2$, $^5G_6$ and $^5D_4$. We have tried to include the $^5L_6$ level into the calculations, but because this level is not in resonance with the ligand levels it has no effect on the results.

In order to get the transfer rates and quantum yields several

Table 1 Experimental and theoretical energies (cm^{-1}) of the transitions to the singlet and from the triplet states. Log ε and theoretical oscillator strengths for the transitions to the singlet states are given in parentheses

	Singlet state		Triplet state	
Compound	Experimental[a] Ln = Eu	Theoretical Ln = Eu	Experimental[b] Ln = La	Theoretical Ln = Eu
$[Ln(NO_3)_3L(MeOH)]$	32 723 (4.33) 29 052 (4.37)	29 425 (0.55)	20 852 19 579 18 434	20 015
$[Ln(L)_3]^{3+}$	33 450 (4.77) 27 700 (4.69)	30 992 (0.71) 30 964 (0.70)	20 893 19 608 18 485	20 958

[a] Absorption spectra in CH_3CN at 293 K; 1 : 1 complex: ref. 20, 1 : 3 complex: ref. 9. [b] Emission spectra of frozen solutions in CH_3CN (77 K), ref. 4.

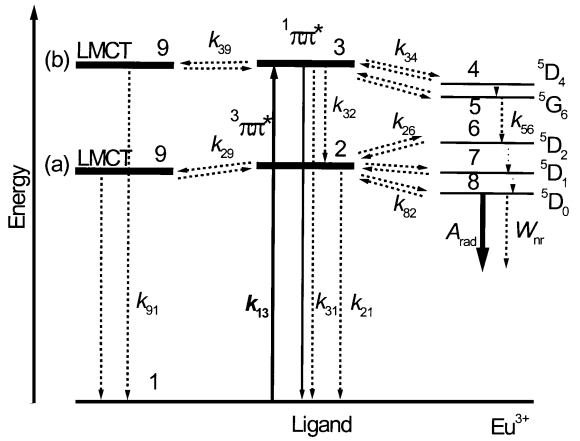

Fig. 2 Diagram of the most probable states to be involved in the energy transfer process in $[Eu(NO_3)_3L(MeOH)]$ and $[Eu(L)_3]^{3+}$, with their numbering scheme. The solid and dashed arrows represent radiative (rate A_{rad}) and non-radiative (rate W_{nr}) processes, respectively. The diagram also shows how the LMCT state is taken into consideration: close to (a) the triplet and (b) the singlet states of the ligand.

parameters are needed, which were obtained from the experimental structures and from spectroscopic calculations. For $[Eu(NO_3)_3L(MeOH)]$, the following parameters were used: $R_L = 4.3$ Å (calculated by using eqn. (9) of ref. 12), $\gamma_{triplet} = 3100\ cm^{-1}$, $A_{rad} = 514\ s^{-1}$, taken as the sum of the spontaneous emission coefficients of the transitions $^5D_0 \rightarrow {}^7F_{0,1,2,4}$;[20] $\tau^{-1}(^5D_0) = 1053\ s^{-1}$;[20] the theoretical value of the z-component of the electric dipole matrix element in eqn. (3) is 1.91×10^{-36} (esu)^2 cm^2; the dipole–dipole contribution to the transfer rates was calculated by using the following theoretical values for Ω_λ^{ed} (in 10^{-20} cm^2): $\Omega_2^{ed} = 0.20$, $\Omega_4^{ed} = 0.45$ and $\Omega_6^{ed} = 0.49$. For $[Eu(L)_3]^{3+}$, the following parameters were taken: $R_L = 5.12$ Å, $\gamma_{triplet} = 3300\ cm^{-1}$, $A_{rad} = 484\ s^{-1}$,[9] $\tau^{-1}(^5D_0) = 2083\ s^{-1}$;[9] the theoretical value of the z-component of the electric dipole matrix element is 4.0×10^{-36} (esu)^2 cm^2;† the dipole–dipole contribution for the transfer rates was calculated using $\Omega_2^{ed} = 0.25$, $\Omega_4^{ed} = 0.39$ and $\Omega_6^{ed} = 0.55$ (in 10^{-20} cm^2). For both complexes, a value of $10^6\ s^{-1}$ was assumed for all the non-radiative decay rate among the 4f–4f transitions. The screening factors were taken as: $\sigma_0 = 0.985$, $\sigma_2 = 0.6$, $\sigma_4 = 0.139$ and $\sigma_6 = -0.1$. The back-transfer rates were obtained by multiplying the energy transfer rate by the Boltzmann factor $e^{-|\Delta|/k_BT}$ at room temperature. The direct transfer rate to the $^5D_0$ level was calculated assuming (i) a factor of thermal population equal to 0.17, at 300 K, for the $^7F_1$ manifold corresponding to a mean energy difference of 370 cm^{-1} between $^7F_1$ and $^7F_0$ (exp.: 374 and 370 cm^{-1} for the 1 : 1 and 1 : 3 complexes, respectively) of and (ii) an energy difference $\Delta = E(\text{triplet}) - [E(^5D_0) - E(^7F_1)]$.

Table 2 presents the energy transfer and back-transfer rates for the two modelled compounds. The arrows indicate the direction of the energy transfer. The energy transfer rates are larger for the $^5D_0$ and $^5D_1$ levels, for which the exchange mechanism dominates, than for the higher excited 4f levels, for which the multipolar mechanisms are the most important ones.

Typical values of the remaining transfer rates were assumed to be identical to those found for co-ordination compounds in the solid state, namely, $k_{13} = \theta = 10^4$, $k_{21} = 10^5$, $k_{32} = 10^8$ and $k_{31} = 10^6\ s^{-1}$.[7] In solution, which is the present case, the k_{31} and k_{21} rates may have higher values than in the solid state, because higher collision rates between the complexes and the solvent molecules at room temperature provide additional quenching pathways.[21–23] In the calculations, we assumed a quite high k_{32} rate (in the range 10^7–$10^9\ s^{-1}$), as

† 1 esu = 3 33564 × 10^{-10} C.

Table 2 Calculated energy transfer rates (s^{-1})

Ligand state/cm^{-1}	4f state/cm^{-1}	Transfer rate/s^{-1}	Back-transfer rate/s^{-1}
$[Eu(NO_3)_3L(MeOH)]$			
Triplet (19 622) →	$^5D_0$ (17 300)	$k_{28} = 1.47 \times 10^8$	$k_{82} = 5.51 \times 10^2$
Triplet (19 622) →	$^5D_1$ (19 070)	$k_{27} = 7.29 \times 10^8$	$k_{72} = 5.25 \times 10^7$
Triplet (19 622) ←	$^5D_2$ (21 500)	$k_{62} = 3.78 \times 10^6$	$k_{26} = 4.91 \times 10^2$
Singlet (28 785) →	$^5G_6$ (26 750)	$k_{35} = 1.80 \times 10^7$	$k_{53} = 1.11 \times 10^3$
Singlet (28 785) →	$^5D_4$ (27 600)	$k_{34} = 6.61 \times 10^6$	$k_{43} = 2.33 \times 10^4$
$[Eu(L)_3]^{3+}$			
Triplet (19 662) →	$^5D_0$ (17 300)	$k_{28} = 9.04 \times 10^7$	$k_{82} = 2.80 \times 10^2$
Triplet (19 662) →	$^5D_1$ (19 070)	$k_{27} = 2.67 \times 10^9$	$k_{72} = 1.59 \times 10^8$
Triplet (19 662) ←	$^5D_2$ (21 500)	$k_{62} = 5.63 \times 10^5$	$k_{26} = 0.89 \times 10^2$
Singlet (27 700) →	$^5G_6$ (26 750)	$k_{35} = 8.37 \times 10^6$	$k_{53} = 9.06 \times 10^4$
Singlet (27 700) →	$^5D_4$ (27 600)	$k_{34} = 2.67 \times 10^6$	$k_{43} = 1.65 \times 10^6$

observed for lanthanide co-ordination compounds and resulting from the heavy-atom effect.[24,25] Therefore, in the numerical solution of the rate equations, several values of k_{21}, k_{31}, and k_{32} were tested in order to determine the dependence of the populations in the stationary regime upon these rates and to establish their optimum values. The numerical solutions of the rate equations were used to perform a sensitivity variable analysis, that is to investigate how the variation of the rates (k_{ij}) affects the quantum yield. These populations were then introduced in eqn. (7) to calculate the emission quantum yield of the compounds, whose values are presented in Table 3.

It is noteworthy that the emission quantum yield is highly dependent upon k_{21}, k_{31}, and k_{32}. A quite satisfactory match between the calculated and experimental quantum yield for $[EuL(NO_3)_3(MeOH)]$ was found by setting $k_{21} = 10^9$, $k_{31} = 10^8$ and $k_{32} = 10^8\ s^{-1}$ (calculated quantum yield = 2.67% and experimental quantum yield = 2.8%), indicating that non-radiative rates in the ligand are indeed very high for this compound in solution. The value obtained for k_{21} is in good agreement with experimental data reported for trivalent lanthanide chelates in solution.[21] This high value is indeed expected, since the $[Eu(NO_3)_3L(MeOH)]$ and $[Eu(L)_3]^{3+}$ compounds do not display ligand phosphorescence at room temperature.[22] For $[Eu(L)_3]^{3+}$, no satisfying set of rate constants could be found to reproduce the experimental quantum yield, indicating the existence of one or more additional quenching mechanisms. Since the existence of a low-lying ligand-to-metal charge-transfer state was postulated to explain the extremely low quantum yield for $[Eu(L)_3]^{3+}$,[4] we have carried

Table 3 Calculated quantum yield (%) at 300 K for several values of the transition rates

			Quantum yield	
k_{31}/s^{-1}	k_{21}/s^{-1}	k_{32}/s^{-1}	$[Eu(NO_3)_3L(MeOH)]$	$[Eu(L)_3]^{3+}$
10^5	10^5	10^8	75.6	23.2
10^6	10^5	10^8	75.1	23.0
10^7	10^5	10^8	70.0	21.2
10^8	10^5	10^8	41.2	12.1
10^9	10^5	10^8	5.47	2.12
10^6	10^6	10^8	74.3	22.8
10^6	10^7	10^8	67.5	20.8
10^6	10^8	10^8	35.1	11.2
10^6	10^9	10^8	5.16	1.89
10^6	10^5	10^7	73.5	22.0
10^6	10^5	10^9	75.6	23.2
10^8	10^9	10^8	2.67	0.97
10^9	10^9	10^7	0.144	0.0336
Experimental			2.8	8.2×10^{-5}

Table 4 Calculated quantum yield (%) for several values of the k_{39}, k_{31}, and k_{32} rates in $[Eu(L)_3]^{3+}$ at 300 K

k_{39}/s^{-1} ($^1\pi\pi^* \rightarrow$ LMCT)	Quantum yield[a]	Quantum yield[b]
0	0.97	0.034
10^8	0.64	0.030
5×10^8	0.28	0.022
10^9	0.16	0.017
5×10^9	0.037	5.6×10^{-3}
8×10^9	0.024	3.7×10^{-3}
10^{10}	0.019	3.1×10^{-3}
3×10^{10}	6.4×10^{-3}	1.1×10^{-3}
5×10^{10}	3.9×10^{-3}	6.6×10^{-4}
8×10^{10}	2.4×10^{-3}	4.2×10^{-4}
10^{11}	1.9×10^{-3}	3.3×10^{-4}
5×10^{11}	3.9×10^{-4}	6.7×10^{-5}
10^{12}	1.9×10^{-4}	3.4×10^{-5}
Experimental	8.2×10^{-5}	

[a] $k_{31} = 10^8$, $k_{21} = 10^9$, and $k_{32} = 10^8$ s^{-1}. [b] $k_{31} = 10^9$, $k_{21} = 10^9$, and $k_{32} = 10^7$ s^{-1}.

out calculation taking this state into account. Two situations were considered. The first one corresponds to the LMCT state close to the triplet state, while the second one corresponds to the LMCT state close to the singlet state. In both situations the quantum yield was estimated for several values of k_{39} ($^1\pi\pi^* \rightarrow$ LMCT) and k_{29} ($^3\pi\pi^* \rightarrow$ LMCT), while the other rates were kept constant: $k_{91} = 10^9$, $k_{92} = 10^6$, and $k_{93} = 10^6$ s^{-1}. The numeric solutions of the rate equations were obtained by using two sets of k_{ij}: (i) $k_{31} = 10^8$, $k_{21} = 10^9$, and $k_{32} = 10^8$ s^{-1}, and (ii) $k_{31} = 10^9$, $k_{21} = 10^9$, and $k_{32} = 10^7$ s^{-1}. These values were chosen because set (i) is efficient in reproducing the experimental data for $[Eu(NO_3)_3L(MeOH)]$ while set (ii) presents a k_{31} rate higher than in the other set to account for the experimental observation that indeed k_{31} is larger in the 1 : 3 compound than in the 1 : 1 complex.[4] Set (ii) presents also a smaller k_{32} rate, as expected for compounds having extremely low quantum yields, since in this case the triplet state which is generally the most efficient sensitiser for the Eu^{3+} and Tb^{3+} luminescence,[23] should be very little populated. A good fit could only be obtained for the situation where the LMCT state is close to the singlet state and the quantum yields obtained for the steady-state populations are listed in Table 4. The main result lies in the fact that the introduction of the LMCT state indeed causes a large decrease in the emission quantum yield of the triple helical complex. As expected, the 2nd set of k_{ij} results in smaller values of the quantum yield.

The variation of the quantum yield with k_{39} is presented on Fig. 3. The quantum yield decreases considerably for $k_{39} > 10^9$ s^{-1} and a good agreement with the experimental value is found for k_{39} in the range 10^{11} to 5×10^{11} s^{-1}, showing the efficient quenching of the luminescence by the LMCT state. These calculations substantiate the hypothesis postulated on the basis of electrochemical data.[4]

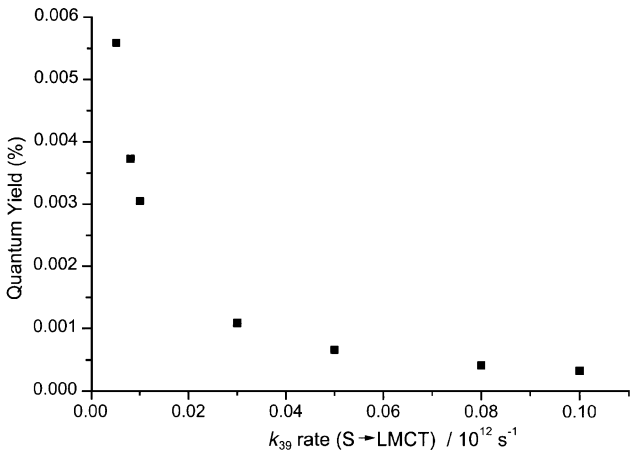

Fig. 3 Calculated quantum yield *vs.* energy transfer rate from the singlet to LMCT state (k_{39}).

Conclusion

The numeric solution of the rate equations indicates high k_{21} and k_{31} rates for the non-radiative deactivation of both 1 : 1 and 1 : 3 complexes in solution. In addition, it clearly points to the presence of a LMCT state with an energy close to that of the singlet state in $[Eu(L)_3]^{3+}$ causing a drastic decrease in the Eu-centred luminescence, contrary to $[Eu(NO_3)_3L]$. Presently, our interest focuses on the theoretical determination of the energy of the charge transfer state and of its influence on the quantum yield. Indeed, the approach presented here is versatile and its ability to predict the quantum yield as a function of the interaction between the LMCT state and $^1\pi\pi^*$ and/or $^3\pi\pi^*$ states opens interesting perspectives for the predictive design of luminescent probes and materials.

Acknowledgements

The authors acknowledge CNPq, FINEP, and PADCT (Brazilian agencies) and the Swiss National Science Foundation for financial support.

References

1 P. Porcher, in *Rare Earths*, ed. R. Saez Puche and P. Caro, Editorial Complutense, Madrid, 1998, p. 43ff.
2 I. Hemmilä, T. Ståhlberg and P. Mottram, *Bioanalytical Applications of Labelling Technologies*, Wallac Oy, Turku, Finland, 1995.
3 G. Mathis, in *Rare Earths*, ed. R. Saez Puche and P. Caro, Editorial Complutense, Madrid, 1998, p. 285ff.
4 S. Petoud, J.-C. G. Bünzli, T. Glanzman, C. Piguet, Q. Xiang and R. P. Thummel, *J. Lumin.*, 1999, **82**, 69.
5 O. L. Malta, *J. Lumin.*, 1997, **71**, 229.
6 F. R. Gonçalves e Silva and O. L. Malta, *J. Alloys Compd.*, 1997, **250**, 427.
7 O. L. Malta, F. R. Gonçalves e Silva and R. Longo, *Chem. Phys. Lett.*, 1999, **307**, 518.
8 C. Piguet, A. F. Williams, G. Bernardinelli, E. Moret and J.-C. G. Bünzli, *Helv. Chim. Acta*, 1992, **75**, 1697.
9 C. Piguet, A. F. Williams, G. Bernardinelli and J.-C. G. Bünzli, *Inorg. Chem.*, 1993, **32**, 4139.
10 J. E. Ridley and M. C. Zerner, *Theor. Chim. Acta*, 1973, **32**, 111.
11 M. C. Zerner, *ZINDO Manual*, QTP, University of Florida, Gainesville, FL, 1990.
12 O. L. Malta and F. R. Gonçalves e Silva, *Spectrochim. Acta, Part A*, 1998, **54**, 1593.
13 W. T. Carnall, H. Crosswhite and H. M. Crosswhite, *Energy Structure and Transition Probabilities of the Trivalent Lanthanides in LaF_3*, Argonne National Laboratory Report, unnumbered, 1977.
14 O. L. Malta, H. F. Brito, J. F. S. Menezes, F. R. Gonçalves e Silva, S. Alves, Jr., F. S. Farias, Jr. and A. M. V. de Andrade, *J. Lumin.*, 1997, **75**, 1.
15 F. R. Gonçalves e Silva, PhD Dissertation, DQF-UFPE, Brazil, 1999; F. R. Gonçalves e Silva, Masters Dissertation, DQF-UFPE, Brazil, 1995.
16 A. V. M. de Andrade, R. L. Longo, A. M. Simas and G. F. de Sá, *J. Chem. Soc., Faraday Trans.*, 1996, **92**, 1835.
17 A. R. Edmonds, *Angular Momentum in Quantum Mechanics*, Princeton University Press, New Jersey, 1975.
18 D. J. Newman and D. C. Price, *J. Phys. C: Solid State Phys.*, 1975, **8**, 2985.
19 M. Faucher and D. Garcia, *Phys. Rev. B*, 1982, **26**, 5451.
20 S. Petoud, J.-C. G. Bünzli, K. J. Schenk and C. Piguet, *Inorg. Chem.*, 1997, **36**, 1345.
21 W. R. Dawson, J. L. Kropp and M. W. Windsor, *J. Chem. Phys.*, 1966, **45**, 2410.
22 N. Filipescu and N. McAvoy, *J. Inorg. Nucl. Chem.*, 1966, **28**, 253.
23 R. D. Archer, H. Chen and L. C. Thompson, *Inorg. Chem.*, 1998, **37**, 2089.
24 C. M. Rudzinski, D. S. Engebretson, W. K. Hartmann and D. G. Nocera, *J. Phys. Chem. A*, 1998, **102**, 7442.
25 G. E. Buono-Core and H. Li, *Coord. Chem. Rev.*, 1990, **99**, 55.